

Adjusting optical cavity birefringence with wavelength tunable laser for axion searches

Hinata Takidera,¹ Hiroki Fujimoto,¹ Yuka Oshima,¹ Satoru Takano,^{1,2} Kentaro Komori,^{1,3}
Tomohiro Fujita,^{4,3,5} Ippei Obata,^{5,6} Masaki Ando,^{1,3} and Yuta Michimura^{3,5}

¹*Department of Physics, The University of Tokyo, Bunkyo, Tokyo 113-0033, Japan*

²*Max-Planck-Institut für Gravitationsphysik (Albert-Einstein-Institut), D-30167 Hannover, Germany*

³*Research Center for the Early Universe (RESCEU), Graduate School of Science,
The University of Tokyo, Bunkyo, Tokyo 113-0033, Japan*

⁴*Department of Physics, Ochanomizu University, Bunkyo, Tokyo 112-8610, Japan*

⁵*Kavli Institute for the Physics and Mathematics of the Universe (Kavli IPMU),
WPI, UTIAS, The University of Tokyo, Kashiwa, Chiba 277-8568, Japan*

⁶*Theory Center, Institute of Particle and Nuclear Studies (IPNS),
High Energy Accelerator Research Organization (KEK), 1-1 Oho, Tsukuba, Ibaraki 305-0801, Japan*

Axions have attracted attention as promising candidates for dark matter (DM). Although axions have been intensively searched for, they have not been observed yet. Recently, novel experiments to search for axion DM have been proposed that use optical cavities to amplify polarization rotation of laser light induced by the axion-photon interaction. One such experiment employs a ring cavity composed of four mirrors. However, its sensitivity to the axion-photon coupling $g_{a\gamma}$ in the low axion mass region is limited due to a reflection phase difference between s- and p-polarizations. In this paper, we propose a new method to improve the sensitivity using zero-phase shift mirrors and a wavelength tunable laser. Moreover, the laser makes it easier to scan the high axion mass region by tuning the reflection phase difference between s- and p-polarizations. We experimentally confirmed that the phase difference generated upon reflection on a zero phase shift mirror satisfies the requirement of 8.6×10^{-3} deg, which corresponds to the half width at half maximum (HWHM) of the p-polarization with the mirror fixed on a folded cavity and a wavelength tunable laser.

I. INTRODUCTION

Axions are one of the leading candidates for dark matter (DM) [1–3]. They were originally proposed to solve the strong CP problem in quantum chromodynamics [4], and are generally called the QCD axion. String theory and supergravity suggest the existence of axion-like particles (ALPs) with a wide range of mass [5, 6]. Although ALPs do not solve the strong CP problem, they are nonetheless well-motivated candidates for DM. In this paper, we collectively call the QCD axion and ALPs as “axions”.

Axions are ultralight particles that weakly interact with photons, electrons, protons, and neutrons. Many experiments have searched for axions utilizing the axion-photon interaction with magnetic field. For example, Axion haloscopes [7, 8] (ADMX [9–12], ADMX SLIC [13]), Axion helioscopes [14] (Sumico [15, 16], CAST [17, 18]), Light shining through a wall experiments [19, 20] (ALPS [21, 22], OSQAR [23]), PVLAS experiment [24], measurements of magnetic field oscillations under static magnetic field (ABRACADABRA [25, 26], SHAFT [27]), astronomical observations (SN1987A [28, 29], M87 [30], NGC1275 [31], H1821+643 [32], Pulsars [33], Axion star explosions [34], CMB [35], MWD Polarization [36], M82 [37]), and Earth’s magnetic fields (SNIPE [38], SuperMAG [39, 40], Eskdalemuir [41]) have set upper limits. Although axions have been intensively searched for, they have not been discovered yet.

Recently, novel experiments to search for axion DM have been proposed that utilize the axion-photon interaction without magnetic field. These experiments aim

to detect a phase velocity difference between left- and right-handed circularly polarized light using an optical cavity [42]. When the basis of circularly polarized light is converted to that of linearly polarized light, it can be regarded as a polarization rotation. Gravitational wave detectors can be used to search for axion DM by detecting the polarization rotation [43]. In this method, using the arm cavity reflection ports of gravitational wave detectors degrades the sensitivity to the axion-photon coupling in the low axion mass region due to the flip of the polarization plane upon reflection on the mirror. On the other hand, using the arm cavity transmission ports of gravitational wave detectors improves the sensitivity to the axion-photon coupling in the low axion mass region since photons travel in the cavity for odd-number of times [44]. LIDA [45] and ADBC experiment [46, 47] are laser-interferometric detectors with ring cavities searching for axion DM. The ring cavity prevents cancellation of the polarization rotation angle caused by the flip of the polarization plane upon reflection on the mirror. LIDA [45] and ADBC experiment [47] have searched for axion DM near 2 neV and 50 neV, respectively.

We proposed Dark matter Axion search with riNg Cavity Experiment (DANCE) [48]. We inject linearly polarized light into a bow-tie ring cavity and amplify the polarization rotation angle due to the axion-photon interaction. One of the main challenges faced by experiments using a ring cavity is that the resonant frequency difference between s- and p-polarizations degrades the sensitivity in the low axion mass region [45, 47, 49], in contrast to experiments using a linear cavity such as [42], [43], and [44]. The parity inversion caused by mirror re-

flexion leads to a redefinition of the polarization axis. Independent of this effect, the reflection phase difference between s- and p-polarizations induced upon reflection is ideally 0 deg. However, due to the dielectric multi-layer coating of the mirror, this phase difference shifts from 0 deg, leading to the resonant frequency difference between s- and p-polarizations. This degrades the sensitivity to the axion-photon coupling in the low axion mass region. The detail is described in Section II. We refer to it as a non-simultaneous resonance when the resonant frequency difference between s- and p-polarizations is not 0 Hz, and as a simultaneous resonance when the difference is 0 Hz. In order to conduct a sensitive axion DM search in the low axion mass region, achieving simultaneous resonance is essential. According to the theoretical calculation of the mirror coating, the reflection phase difference between s- and p-polarizations generated by mirror reflection depends on both the angle of incidence on the mirror and the laser wavelength. One approach to achieving simultaneous resonance is tuning the phase difference by adjusting the angle of incidence through mirror rotation [46]. However, the results have some gaps in the searched axion mass range due to manually rotating the mirrors [47]. To search over a wide axion mass range, the mirrors need to be linearly actuated with an accuracy on the order of 0.1 mm. The other approach is using an auxiliary cavity [50]. In this method, the p-polarization is resonant with a ring cavity, and the s-polarization is resonant with a ring cavity and an auxiliary cavity. The auxiliary cavity compensates for the resonant frequency difference between s- and p-polarizations. We presented a method to achieve simultaneous resonance by incorporating an auxiliary cavity to a bow-tie ring cavity [51]. However, the optical loss generated on the polarizing beam splitter (PBS) between the bow-tie ring cavity and the auxiliary cavity degraded the sensitivity.

In this paper, we propose a new method for a broadband and sensitive axion DM search. The approach is to use zero phase shift mirrors and a wavelength tunable laser. We can tune the reflection phase difference between s- and p-polarizations by varying the laser wavelength, without the need for an auxiliary cavity. In this work, we designed a folded cavity to demonstrate a proof of principle for simultaneous resonance and to evaluate the reflection phase difference between s- and p-polarizations per mirror with the zero-phase shift mirror and the wavelength tunable laser. In Section II, we describe the principle of axion DM search and the reflection phase difference between s- and p-polarizations. Section III outlines the concept and setup of our experiment. In Section IV and V, we present and discuss the results of this work. Finally, Section VI provides the conclusion. In this paper, we set the natural unit system, $\hbar = c = 1$, unless otherwise noted.

II. PRINCIPLE

Assuming that DM is composed of ALPs, due to its large number density, the axion field $a(t)$ behaves like a classical wave with axion mass m_a , and is expressed by

$$a(t) = a_0 \cos(m_a t + \delta_\tau(t)), \quad (1)$$

where a_0 is the axion field amplitude and $\delta_\tau(t)$ is the phase factor. The axion field oscillate with a frequency f_a , which is related to the axion mass m_a by $f_a = m_a/(2\pi) = 242 \text{ Hz} (m_a/10^{-12} \text{ eV})$. $\delta_\tau(t)$ stays constant during the coherent time $\tau = \lambda_a/v_a = 2\pi/m_a v_a^2$, where $\lambda_a = 2\pi/m_a v_a$ is the de Broglie wavelength of axion DM, $v_a \sim 10^{-3}$ is the galactic virial velocity of axion DM [52]. The phase velocity of left- and right-handed circularly polarized light is given by

$$c_{L/R}(t) = 1 \pm \delta c_0 \sin(m_a t + \delta_\tau(t)), \quad (2)$$

$$\delta c_0 \equiv \frac{g_{a\gamma} \sqrt{2\rho_a}}{2k_0}, \quad (3)$$

where $g_{a\gamma}$ is the axion-photon coupling, $\rho_a \equiv m_a^2 a_0^2/2 \sim 0.4 \text{ GeV cm}^{-3}$ is the energy density of axion DM in the solar system [53, 54], and k_0 is the wave number of laser light.

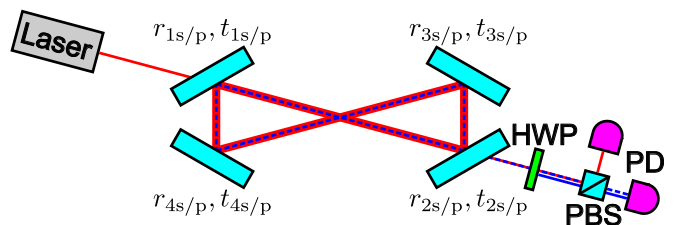


FIG. 1. Configuration of DANCE. The red and blue solid lines indicate s- and p-polarization, respectively. The blue dashed line represents the p-polarization generated via the axion-photon interaction. $r_{js/p}$ ($j = 1, 2, 3, 4$) and $t_{js/p}$ ($j = 1, 2, 3, 4$) are the amplitude reflectivity and transmissivity for s- and p-polarization of the j th mirror, respectively. HWP: Half-wave plate, PBS: Polarizing beam splitter, PD: Photo detector.

Recently, we developed Dark matter Axion search with riNg Cavity Experiment (DANCE) [49]. If we transform the basis of circularly polarized light to that of linearly polarized light, it is interpreted as a polarization rotation. When the polarization is adjusted to s-polarization, the polarization rotation induces p-polarization sidebands. In the following, we consider linearly polarized light. When we inject s-polarization into the cavity as shown in Fig. 1, the electric field of the transmitted light $\mathbf{E}_t(t)$ is given by

$$\mathbf{E}_t(t) = \frac{t_{1s}t_{2s}e^{-ik_0l_1}}{1 - r_{1s}r_{4s}r_{3s}r_{2s}e^{-ik_02(l_1+l_2)}} E_0 e^{i\omega_0 t} \begin{pmatrix} \mathbf{e}_s & \mathbf{e}_p \end{pmatrix} \begin{pmatrix} 1 \\ -\delta\phi(t) \end{pmatrix}, \quad (4)$$

$$\delta\phi(t) \equiv \int_{-\infty}^{\infty} \frac{d\omega}{2\pi} \tilde{\delta c}(\omega) e^{i\omega t} H_a(\omega), \quad (5)$$

where l_1 is the long side of the cavity length, l_2 is the short side of the cavity length, E_0 is the electric field of the laser light, ω_0 is the angular frequency of the laser light, \mathbf{e}_s and \mathbf{e}_p are the basis vectors for s- and p-polarization, respectively, $\delta\phi(t)$ is the polarization ro-

tation angle of the transmitted light, $\tilde{\delta c}(\omega)$ is the Fourier transform of $\delta c(t)$, and $H_a(\omega)$ is the transfer function from $\tilde{\delta c}(\omega)$ to the Fourier transform of $\delta\phi(t)$. When s-polarization is resonant in the cavity, $k_0 2(l_1 + l_2) = 2n\pi$, the transfer function $H_a(\omega)$ is given by

$$H_a(\omega) = k_0 \sqrt{\frac{1 - |r_{2p}|^2}{1 - |r_{2s}|^2}} \frac{1}{i\omega(1 - r_{1p}r_{4p}r_{3p}r_{2p}e^{-i\omega 2(l_1+l_2)})} \left[-(1 - e^{-i\omega l_2}) \left(r_{1p}r_{4s}r_{3s}r_{2s} + r_{1p}r_{4p}r_{3p}r_{2s}e^{-i\omega(l_1+l_2)} \right) \right. \\ \left. + (1 - e^{-i\omega l_1}) \left(r_{1p}r_{4p}r_{3s}r_{2s}e^{-i\omega l_2} + r_{1p}r_{4p}r_{3p}r_{2p}e^{-i\omega(l_1+2l_2)} \right) \right]. \quad (6)$$

s- and p-polarizations receive reflection phase $\phi_{js/p}$ upon reflection on the j th mirror. We define the reflection phase difference between s- and p-polarizations $\Delta\phi_j = \phi_{js} - \phi_{jp}$ ($j = 1, 2, 3, 4$), and assign this phase difference to r_{jp} . Therefore, r_{js} is a real number, whereas r_{jp} is a complex number, expressed as $r_{jp} = |r_{jp}|e^{i\Delta\phi_j}$. $\Delta\phi_j$ is given by

$$\Delta\phi_j = \frac{2\pi}{\nu_{\text{FSR}}} \Delta\nu_j, \quad (7)$$

where $\nu_{\text{FSR}} = c/2(l_1 + l_2)$, with c being the speed of light, is the free spectral range (FSR) of the cavity, and

$\Delta\nu_j = \nu_{js} - \nu_{jp}$ ($j = 1, 2, 3, 4$) is the resonant frequency difference between s- and p-polarizations.

In order to detect the polarization rotation generated by the axion-photon interaction, as shown in Fig. 1, we use a half-wave plate (HWP) to leak a small amount of the s-polarization into the p-polarization, which acts as a local oscillator (LO) at angular frequency ω_0 [46]. We aim to search for axion DM by detecting the beat signal between the LO and the p-polarization generated by the axion-photon coupling, which oscillates at angular frequency $\omega_0 \pm m_a$. The sensitivity to the axion-photon coupling is limited by quantum shot noise [48]. The signal-to-noise ratio (SNR) is given by [55]

$$\text{SNR} = \frac{P_{t,s} 4\theta_{\text{HWP}} \delta c_0 |H'_a(m_a)|}{\sqrt{2\delta P_{\text{shot}}}} \times \begin{cases} T_{\text{obs}}^{1/2} & (T_{\text{obs}} < \tau), \\ (T_{\text{obs}}\tau)^{1/4} & (\tau < T_{\text{obs}}), \end{cases} \quad (8)$$

$$P_{t,s} \equiv \frac{|t_{1s}t_{2s}|^2}{|1 - r_{1s}r_{4s}r_{3s}r_{2s}|^2} |E_0|^2, \quad (9)$$

$$\delta P_{\text{shot}} \equiv 2\theta_{\text{HWP}} \sqrt{2\hbar\omega_0 P_{t,s}}, \quad (10)$$

$$|H'_a(m_a)| \equiv \frac{1}{2} \sqrt{(\text{Re}[H_a(m_a) + H_a(-m_a)])^2 + (\text{Im}[H_a(m_a) - H_a(-m_a)])^2}, \quad (11)$$

where $P_{t,s}$ is the power of the s-polarized transmitted light, θ_{HWP} is the rotation angle of the HWP, $H'_a(m_a)$ is the transfer function considering the case where the reflection phase difference between s- and p-polarizations is generated upon reflection on the mirrors, δP_{shot} is the

one-sided power spectral density of the shot noise, T_{obs} is the observation time of axion DM, τ is the coherent time of axion DM, and \hbar is the reduced Planck constant. When $T_{\text{obs}} < \tau$, the phase factor $\delta_\tau(t)$ stays constant during τ , and the SNR scales as $T_{\text{obs}}^{1/2}$. In contrast, when

$\tau < T_{\text{obs}}$, $\delta_\tau(t)$ stays constant within each τ , but changes randomly between different τ . Therefore, the SNR scales as $(T_{\text{obs}}\tau)^{1/4}$.

Assuming $\text{SNR} \geq 1$, the axion-photon coupling $g_{a\gamma}$ is given by

$$g_{a\gamma} \geq 1.55 \times 10^{-11} \text{ GeV}^{-1} \frac{|1 - r_{1s}r_{4s}r_{3s}r_{2s}|}{|t_{1s}t_{2s}|} \sqrt{\frac{0.4 \text{ GeV cm}^{-3}}{\rho_a} \frac{1 \text{ W}}{P_{\text{in}}} \frac{1064 \text{ nm}}{\lambda_0} \frac{4.0 \times 10^9 \text{ eV}^{-1}}{|H'_a(m_a)|/k_0}} \times \begin{cases} \left(\frac{1 \text{ year}}{T_{\text{obs}}}\right)^{1/2} & (T_{\text{obs}} < \tau), \\ \left(\frac{1 \text{ year}}{T_{\text{obs}}\tau}\right)^{1/4} & (\tau < T_{\text{obs}}), \end{cases} \quad (12)$$

where $P_{\text{in}} \equiv |E_0|^2$ is the input laser power to the cavity, and λ_0 is the laser wavelength. Figure 2 shows the target sensitivity to the axion-photon coupling of DANCE and the current upper limits obtained from previous research. When $\Delta\phi_j = 0$, we set $|H'_a(m_a)| = |H_a(m_a)|$, enabling a sensitive axion DM search in the low axion mass region. Tuning the laser wavelength to 1065 nm to satisfy $\Delta\phi_j = 0$, simultaneous resonance can be achieved as shown by the blue dotted and red dashed lines in Fig. 2. The first bending point in Fig. 2 is determined by T_{obs} and τ . When $T_{\text{obs}} < \tau$, $g_{a\gamma}$ is flat. In contrast, when $\tau < T_{\text{obs}}$, $g_{a\gamma}$ scales as $m_a^{1/4}$. The second bending point in Fig. 2 corresponds to the half width at half maximum (HWHM) of the p-polarization, given by

$$\nu_{\text{HWHM,p}} = \frac{c}{2L\mathcal{F}_p}, \quad (13)$$

where L is the round-trip of the cavity and \mathcal{F}_p is the finesse of the p-polarization:

$$\mathcal{F}_p = \frac{\pi\sqrt{r_{1p}r_{4p}r_{3p}r_{2p}}}{1 - r_{1p}r_{4p}r_{3p}r_{2p}}. \quad (14)$$

When the axion mass is higher than the mass corresponding to the $\nu_{\text{HWHM,p}}$, $g_{a\gamma}$ scales as $m_a^{5/4}$.

On the other hand, when $\Delta\phi_j \neq 0$, we must use the modified transfer function $H'_a(m_a)$, which degrades the sensitivity to the axion-photon coupling in the low axion mass region. However, it is possible to enhance the sensitivity at the axion mass corresponding to the resonant frequency difference between s- and p-polarizations by tuning the laser wavelength appropriately as shown in Fig. 2. The reflectivity of mirrors depends on the laser wavelength. Therefore, the wavelength needs to be tuned within the range where the reflectivity remains high to prevent the sensitivity degradation. The wavelength can be adjusted up to 1045 nm, which corresponds to the total reflection phase difference between s- and p-polarizations of -25.6 deg, as indicated by the cyan dotted and violet dashed lines in Fig. 2.

III. EXPERIMENT

We describe the concept and setup of our experiment. According to [49], the reflection phase difference between

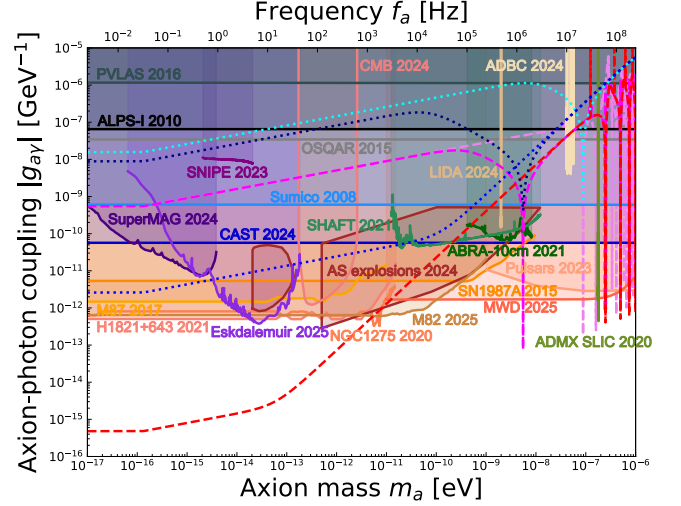


FIG. 2. The dotted and dashed lines represent the target sensitivity based on the parameters listed in Tables I and II. We assume that each mirror has the same reflection phase difference between s- and p-polarizations, $T_{\text{obs}} = 1$ year, and $|r_{js/p}|^2 + |t_{js/p}|^2 = 1$. The blue, navy, and cyan dotted lines correspond to the upper, center, and lower rows of Table I, with the upper row of Table II. The red, magenta, and violet dashed lines correspond to the same rows of Table I, with the lower row of Table II. The colored bands show the current upper limits obtained from ADMX SLIC [13], Sumico [16], CAST [18], ALPS [22], OSQAR [23], PVLAS experiment [24], ABRACADABRA [26], SHAFT [27], SN1987A [29], M87 [30], NGC1275 [31], H1821+643 [32], Pulsars [33], Axion star explosions [34], CMB [35], MWD Polarization [36], M82 [37], SNIPE [38], SuperMAG [40], Eskdalemuir [41], LIDA [45], and ADBC experiment [47].

s- and p-polarizations of each mirror was estimated by dividing the total phase difference from four mirrors by four. In this method, we did not accurately estimate the phase difference. In order to address this issue, we proposed a folded cavity to measure the phase difference as shown in Fig. 3. The cavity is made of a super-invar spacer and consists of the input, end, and test mirrors, all of which are fixed to the spacer by jigs. Table III shows the summary of the folded cavity parameters. Both the input and end mirrors are direct incidence. Incident an-

TABLE I. Values of the laser wavelength λ_0 , the total reflection phase difference between s- and p-polarizations $\Delta\phi_{\text{tot}}$, and the total resonant frequency difference between two polarizations $\Delta\nu_{\text{tot}}$ are shown. The values of $\Delta\phi_{\text{tot}}$ and $\Delta\nu_{\text{tot}}$ are based on the design specifications of the test mirror used in this work.

λ_0	$\Delta\phi_{\text{tot}}$	$\Delta\nu_{\text{tot}}$
1065 nm	0 deg	0 Hz
1064 nm	-1.6 deg	-1.3 MHz
1045 nm	-25.6 deg	-21.3 MHz

TABLE II. Summary of the DANCE parameters.

Parameter	Symbol	Value
Round-trip	$L = 2(l_1 + l_2)$	1 m
Cavity length	(l_1, l_2)	(45 cm, 5 cm)
Input power	P_{in}	1 W
Transmissivity		
1st mirror	$(t_{1s} ^2, t_{1p} ^2)$	(6 ppm, 300 ppm)
2nd mirror	$(t_{2s} ^2, t_{2p} ^2)$	(6 ppm, 300 ppm)
3rd mirror	$(t_{3s} ^2, t_{3p} ^2)$	(6 ppm, 300 ppm)
4th mirror	$(t_{4s} ^2, t_{4p} ^2)$	(6 ppm, 300 ppm)
Round-trip	$L = 2(l_1 + l_2)$	10 m
Cavity length	(l_1, l_2)	(4.5 m, 0.5 m)
Input power	P_{in}	100 W
Transmissivity		
1st mirror	$(t_{1s} ^2, t_{1p} ^2)$	(3.14 ppm, 3.14 ppm)
2nd mirror	$(t_{2s} ^2, t_{2p} ^2)$	(3.14 ppm, 3.14 ppm)
Reflectivity		
3rd mirror	$(r_{3s} ^2, r_{3p} ^2)$	(100%, 100%)
4th mirror	$(r_{4s} ^2, r_{4p} ^2)$	(100%, 100%)

gle on the test mirror is 42 deg, which is the same as that used in [49]. Therefore, we can measure the reflection phase difference between s- and p-polarizations only generated only on the test mirror. Using this setup, we can accurately estimate the phase difference for each mirror in a bow-tie ring cavity, thereby improving the calibration accuracy of the sensitivity.

Long-term measurements of DANCE improve the sensitivity to axion DM. However, if the reflection phase difference between s- and p-polarizations fluctuates during the measurement, the sensitivity will degrade. The requirement for the phase difference per mirror $\Delta\phi_{\text{req}}$, imposed by DANCE with a round-trip length of 1 m is given by

$$|\Delta\phi_{\text{req}} - \Delta\phi_{\text{ave}}| \leq \frac{1}{4} \frac{\nu_{\text{HWHM},p}}{\nu_{\text{FSR}}} \times 360 \text{ deg} = 8.6 \times 10^{-3} \text{ deg}. \quad (15)$$

This requirement is determined using the cavity length and the reflectivity of p-polarization in the upper row of Table II, along with Eq. (13). $\Delta\phi_{\text{ave}}$ is the average value of the reflection phase difference between s- and p-polarizations. We confirmed whether frequency control could be achieved to satisfy this requirement.

In this work, we used a zero phase shift mirror with a wavelength-dependent reflection phase difference between s- and p-polarizations of 0.34 deg/nm. The phase

difference of the mirror is 0 deg at 1065 nm. However, due to manufacturing errors, achieving this exact value is generally difficult. Therefore, it is necessary to use a wavelength tunable laser which can vary the laser wavelength over a wide range, as the cavity is expected to achieve simultaneous resonance at a wavelength different from the design specification. Thus, we employed an external cavity diode laser (ECDL) [56, 57]. Its wavelength tuning range is 1038 nm to 1068 nm.

We conducted two types of experiments to investigate the issues mentioned above. The first experiment aims to probe a wavelength which is able to achieve simultaneous resonance. As shown in upper figure in Fig. 3, the incident laser beam into the cavity was adjusted using a HWP to achieve a 50:50 ratio of s- and p-polarizations. The injected laser power was 10 mW. Applying a triangular wave to the piezo-electric transducer (PZT) of the laser source, we used a PBS to separate the transmitted light into s- and p-polarizations, which were detected with two PDs. The resonant frequency difference between s- and p-polarizations was estimated by fitting the resonant peak with a Lorentzian function. The calibration from the frequency difference $\Delta\nu$ to the reflection phase difference between s- and p-polarizations $\Delta\phi$ is given by

$$\Delta\phi = \frac{\Delta\nu}{\nu_{\text{FSR},\text{folded}}} \times 180 \text{ deg}, \quad (16)$$

where $\nu_{\text{FSR},\text{folded}} = c/2l$ is the FSR of the folded cavity. Since the laser beam reflects twice on the test mirror during a round-trip inside the cavity, it is necessary to divide 360 deg by two. We conducted the above procedure at ten wavelengths in the range of approximately 1064 nm to 1068 nm.

The second experiment aims to evaluate the fluctuations of reflection phase difference between s- and p-polarizations through 24-hour measurement. The lower figure in Fig. 3 shows the experimental setup. In addition to the ECDL, we employed an auxiliary laser to obtain time series data of the beat note between s- and p-polarizations. The polarizations of the ECDL and the auxiliary laser were adjusted to s- and p-polarizations, respectively. The power of the laser beams injected into the cavity was 8 mW for s-polarization and 4 mW for p-polarization. After injecting both laser beams into the cavity, we tuned the wavelengths of both lasers to be identical. However, the wavelength tuning range of the auxiliary laser is limited to 0.3 nm around 1064 nm, so we set the wavelength to 1064.27 nm. Each laser frequency was locked to TEM₀₀ mode using the Pound-Drever-Hall method [58]. In order to suppress laser frequency noise, we designed high-gain filters. The estimated open-loop transfer function gains below 1 Hz are $G_s \sim 7.5 \times 10^5$ for s-polarization and $G_p \sim 5.3 \times 10^5$ for p-polarization. The transmitted light of s-polarization from the ECDL and the reflected light of p-polarization from the auxiliary laser passed through a HWP, and interfered with each other after being projected onto the p-polarization

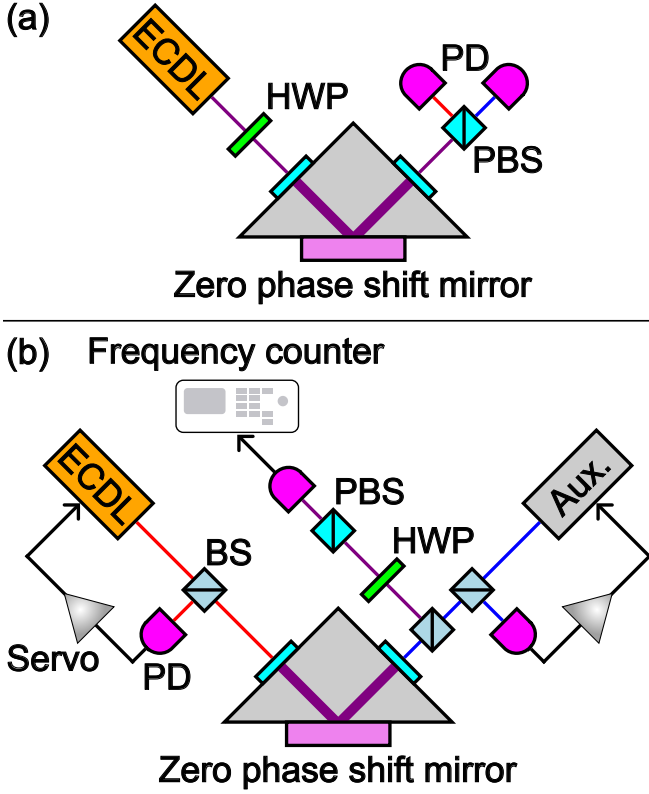


FIG. 3. Schematic of the experimental setup. The red and blue lines represent s- and p-polarization, respectively. The purple line indicates a mixture of s- and p-polarization. (a) Proof of principle for simultaneous resonance. (b) Measurement of the fluctuations of the beat note between s- and p-polarizations. ECDL: External Cavity Diode Laser, BS: Beam splitter.

axis with a PBS. In this setup, signals from other frequency bands, such as the modulation frequency 15 MHz used for frequency control, were mixed into the beat note, distorting its time series data. In order to address this, we used a band-pass filter consisting of passive high-pass and low-pass filters to eliminate unwanted signals, and measured the beat note between s- and p-polarizations with a frequency counter. We recorded the beat note at a sampling rate of 10 Hz for 24 hours.

IV. RESULTS

We present the results of the measurement of the reflection phase difference between s- and p-polarizations. Figure 4 shows the results of wavelength dependence of the phase difference. The error bar on the wavelength represents the resolution of the spectrometer used to measure the laser wavelength, and that on the phase difference indicates the statistical error estimated from ten measurements. The phase difference was $(2.3 \pm 1.1) \times 10^{-3}$ deg at 1066.7 nm and it satisfied the requirement of 8.6×10^{-3} deg. The wavelength was found to be

TABLE III. Summary of the folded cavity parameters, all of which are based on the design specifications.

Parameter	Symbol	Value
Cavity length	l	6 cm
Reflectivity		
Input mirror	$(r_{\text{input},s} ^2, r_{\text{input},p} ^2)$	(99%, 99%)
End mirror	$(r_{\text{end},s} ^2, r_{\text{end},p} ^2)$	(99%, 99%)
Transmissivity		
Test mirror	$(t_{\text{test},s} ^2, t_{\text{test},p} ^2)$	(6 ppm, 300 ppm)
Radius of curvature		
Input mirror	R_1	50 mm
Test mirror	R_2	1000 mm
End mirror	R_3	50 mm
Finesse		
s-polarization	\mathcal{F}_s	312.4
p-polarization	\mathcal{F}_p	303.5

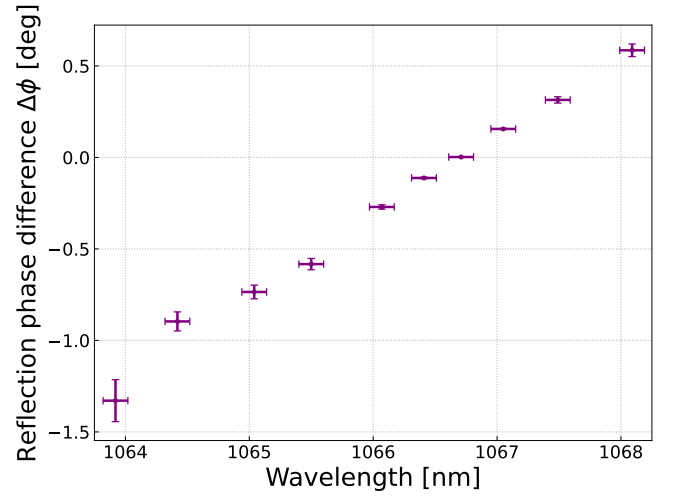


FIG. 4. Wavelength dependence of the reflection phase difference between s- and p-polarizations.

1.7 nm higher than the design specification. The wavelength dependence of the reflection phase difference between s- and p-polarizations is nearly consistent with the design specification. Figure 5 shows the time series data of the beat note between s- and p-polarizations, obtained by calibrating using Eq. (16). The average reflection phase difference between s- and p-polarizations was $\Delta\phi_{\text{ave}} = 0.8306$ deg, and the standard deviation was 1.3×10^{-3} deg. This fluctuation is 6.6 times smaller than the requirement of 8.6×10^{-3} deg.

V. DISCUSSION

We discuss the results of this work. The laser wavelength which satisfies the requirement for reflection phase difference between s- and p-polarizations was shifted from the design specification. We consider this shift to be attributed to the thickness error in the dielectric multi-layer coating of the zero phase shift mirror by manufacturing

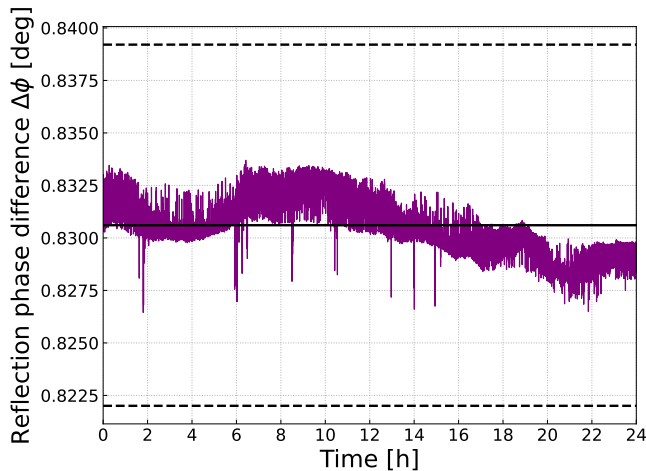


FIG. 5. Time series data of the beat note between s- and p-polarizations. The black solid line indicates the average reflection phase difference between s- and p-polarizations $\Delta\phi_{\text{ave}} = 0.8306$ deg, and the black dashed line represents the requirement range for the phase difference, $\Delta\phi_{\text{ave}} \pm 8.6 \times 10^{-3}$ deg.

error.

We discuss the cause of the beat note fluctuations. Although common mode rejection was expected to be effective, the measured fluctuations were approximately three orders of magnitude larger than the frequency noise. In principle, the fluctuations can be limited by the frequency counter noise. However, they were approximately six orders of magnitude worse than the estimated frequency counter noise. We consider room temperature fluctuations to be one of the causes. They may cause thickness fluctuations in the dielectric multi-layer coating of the zero phase shift mirror, inducing fluctuations in the reflection phase difference between s- and p-polarizations.

VI. CONCLUSION

Novel experiments using optical cavities have been proposed. The first demonstration with the optical ring cavity has already been conducted, revealing that the method limits the sensitivity to the axion-photon coupling in the low axion mass region due to the reflection phase difference between s- and p-polarizations upon reflection on the mirror [45, 47, 49]. In this paper, we propose a new approach for a broadband and sensitive axion DM search. In the low axion mass region, we can improve the sensitivity by achieving simultaneous resonance with a zero phase shift mirror and a wavelength tunable laser. In the high axion mass region, it is possible to search by tuning the laser wavelength to the reflection phase difference between s- and p-polarizations corresponding to the dip frequency.

In this work, we confirmed that the reflection phase difference between s- and p-polarizations satisfied the requirement imposed by DANCE with a round-trip length of 1 m. Therefore, we demonstrated a proof of principle for simultaneous resonance and successfully evaluated the phase difference per mirror using the folded cavity, the zero phase shift mirror, and the wavelength tunable laser. The mirror evaluation method developed in this work improves the calibration accuracy for the sensitivity in axion DM searches using optical ring cavities.

ACKNOWLEDGEMENT

We would like to thank Shigemi Otsuka and Togo Shimozaawa for manufacturing some parts, and Kenichi Nakagawa for providing detailed instructions on the use and assembly of the ECDL. This work is supported by JSPS KAKENHI Grant Nos. 19K14702, 20H05850, 20H05854, 20H05859, 20H05639, 24K00640, and 24K21546, and by JST FOREST Program No. JPMJFR222Y.

-
- [1] J. Preskill, M. B. Wise, and F. Wilczek, *Phys. Lett. B* **120**, 127 (1983).
 - [2] L. Abbott and P. Sikivie, *Phys. Lett. B* **120**, 133 (1983).
 - [3] M. Dine and W. Fischler, *Phys. Lett. B* **120**, 137 (1983).
 - [4] R. D. Peccei and H. R. Quinn, *Phys. Rev. Lett.* **38**, 1440 (1977).
 - [5] P. Svrcek and E. Witten, *J. High Energy Phys.* **2006** (06), 051.
 - [6] A. Arvanitaki, S. Dimopoulos, S. Dubovsky, N. Kaloper, and J. March-Russell, *Phys. Rev. D* **81**, 123530 (2010).
 - [7] P. Sikivie, *Phys. Rev. Lett.* **51**, 1415 (1983).
 - [8] S. Asztalos, E. Daw, H. Peng, L. J. Rosenberg, C. Hagmann, D. Kinion, W. Stoeffl, K. van Bibber, P. Sikivie, N. S. Sullivan, D. B. Tanner, F. Nezrick, M. S. Turner, D. M. Moltz, J. Powell, *et al.*, *Phys. Rev. D* **64**, 092003 (2001).
 - [9] S. J. Asztalos, G. Carosi, C. Hagmann, D. Kinion, K. van Bibber, M. Hotz, L. J. Rosenberg, G. Rybka, J. Hoskins, J. Hwang, P. Sikivie, D. B. Tanner, R. Bradley, and J. Clarke, *Phys. Rev. Lett.* **104**, 041301 (2010).
 - [10] N. Du, N. Force, R. Khatiwada, E. Lentz, R. Ottens, L. J. Rosenberg, G. Rybka, G. Carosi, N. Woollett, D. Bowring, A. S. Chou, A. Sonnenschein, W. Wester, C. Boutan, N. S. Oblath, *et al.* (ADMX Collaboration), *Phys. Rev. Lett.* **120**, 151301 (2018).
 - [11] T. Braine, R. Cervantes, N. Crisosto, N. Du, S. Kimes, L. J. Rosenberg, G. Rybka, J. Yang, D. Bowring, A. S. Chou, R. Khatiwada, A. Sonnenschein, W. Wester, G. Carosi, N. Woollett, *et al.* (ADMX Collaboration), *Phys. Rev. Lett.* **124**, 101303 (2020).
 - [12] C. Bartram, T. Braine, E. Burns, R. Cervantes, N. Crisosto, N. Du, H. Korandla, G. Leum, P. Mohapatra, T. Nitta, L. J. Rosenberg, G. Rybka, J. Yang, J. Clarke, I. Siddiqi, *et al.* (ADMX Collaboration), *Phys. Rev. Lett.* **127**, 261803 (2021).

- [13] N. Crisosto, P. Sikivie, N. S. Sullivan, D. B. Tanner, J. Yang, and G. Rybka, *Phys. Rev. Lett.* **124**, 241101 (2020).
- [14] D. M. Lazarus, G. C. Smith, R. Cameron, A. C. Melissinos, G. Ruoso, Y. K. Semertzidis, and F. A. Nezrick, *Phys. Rev. Lett.* **69**, 2333 (1992).
- [15] S. Moriyama, M. Minowa, T. Namba, Y. Inoue, Y. Takasu, and A. Yamamoto, *Phys. Lett. B* **434**, 147 (1998).
- [16] Y. Inoue, Y. Akimoto, R. Ohta, T. Mizumoto, A. Yamamoto, and M. Minowa, *Phys. Lett. B* **668**, 93 (2008).
- [17] V. Anastassopoulos, S. Aune, K. Barth, A. Belov, H. Bräuninger, G. Cantatore, J. M. Carmona, J. F. Castel, S. A. Cetin, F. Christensen, J. I. Collar, T. Dafni, M. Davenport, T. A. Decker, A. Dermenev, *et al.* (CAST Collaboration), *Nat. Phys.* **13**, 584 (2017).
- [18] K. Altenmüller, V. Anastassopoulos, S. Argüedas-Cuendis, S. Aune, J. Baier, K. Barth, H. Bräuninger, G. Cantatore, F. Caspers, J. F. Castel, S. A. Çetin, F. Christensen, C. Cogollos, T. Dafni, M. Davenport, *et al.* (CAST Collaboration), *Phys. Rev. Lett.* **133**, 221005 (2024).
- [19] K. Van Bibber, N. R. Dagdeviren, S. E. Koonin, A. K. Kerman, and H. N. Nelson, *Phys. Rev. Lett.* **59**, 759 (1987).
- [20] A. A. Anselm, *Phys. Rev. D* **37**, 2001 (1988).
- [21] K. Ehret, M. Frede, S. Ghazaryan, M. Hildebrandt, E.-A. Knabbe, D. Kracht, A. Lindner, J. List, T. Meier, N. Meyer, D. Notz, J. Redondo, A. Ringwald, G. Wiedemann, and B. Willke, *Nucl. Instrum. Methods Phys. Res. A* **612**, 83 (2009).
- [22] K. Ehret, M. Frede, S. Ghazaryan, M. Hildebrandt, E.-A. Knabbe, D. Kracht, A. Lindner, J. List, T. Meier, N. Meyer, D. Notz, J. Redondo, A. Ringwald, G. Wiedemann, and B. Willke, *Phys. Lett. B* **689**, 149 (2010).
- [23] R. Ballou, G. Deferne, M. Finger, M. Finger, L. Flekova, J. Hosek, S. Kunc, K. Macuchova, K. A. Meissner, P. Pugnât, M. Schott, A. Siemko, M. Slunecka, M. Sulc, C. Weinsheimer, *et al.* (OSQAR Collaboration), *Phys. Rev. D* **92**, 092002 (2015).
- [24] F. D. Valle, A. Ejlli, U. Gastaldi, G. Messineo, E. Milotti, R. Pengo, G. Ruoso, and G. Zavattini, *Eur. Phys. J. C* **76** (2016).
- [25] Y. Kahn, B. R. Safdi, and J. Thaler, *Phys. Rev. Lett.* **117**, 141801 (2016).
- [26] C. P. Salemi, J. W. Foster, J. L. Ouellet, A. Gavin, K. M. W. Pappas, S. Cheng, K. A. Richardson, R. Henning, Y. Kahn, R. Nguyen, N. L. Rodd, B. R. Safdi, and L. Winslow, *Phys. Rev. Lett.* **127**, 081801 (2021).
- [27] A. V. Gramolin, D. Aybas, D. Johnson, J. Adam, and A. O. Sushkov, *Nat. Phys.* **17**, 79 (2021).
- [28] J. W. Brockway, E. D. Carlson, and G. G. Raffelt, *Phys. Lett. B* **383**, 439 (1996).
- [29] A. Payez, C. Evoli, T. Fischer, M. Giannotti, A. Mirizzi, and A. Ringwald, *J. Cosmol. Astropart. Phys.* **2015** (02), 006.
- [30] M. D. Marsh, H. R. Russell, A. C. Fabian, B. R. McNamara, P. Nulsen, and C. S. Reynolds, *J. Cosmol. Astropart. Phys.* **2017** (12), 036.
- [31] C. S. Reynolds, M. C. D. Marsh, H. R. Russell, A. C. Fabian, R. Smith, F. Tombesi, and S. Veilleux, *Astrophys. J.* **890**, 59 (2020).
- [32] J. Sisk-Reynés, J. H. Matthews, C. S. Reynolds, H. R. Russell, R. N. Smith, and M. C. D. Marsh, *Mon. Not. R. Astron. Soc.* **510**, 1264 (2021).
- [33] D. Noordhuis, A. Prabhu, S. J. Witte, A. Y. Chen, F. Cruz, and C. Weniger, *Phys. Rev. Lett.* **131**, 111004 (2023).
- [34] M. Escudero, C. K. Pooni, M. Fairbairn, D. Blas, X. Du, and D. J. E. Marsh, *Phys. Rev. D* **109**, 043018 (2024).
- [35] S. Goldstein, F. McCarthy, C. Mondino, J. C. Hill, J. Huang, and M. C. Johnson, *Constraints on axions from patchy screening of the cosmic microwave background* (2024), arXiv:2409.10514 [astro-ph.CO].
- [36] J. N. Benabou, C. Dessert, K. C. Patra, T. G. Brink, W. Zheng, A. V. Filippenko, and B. R. Safdi, *Search for axions in magnetic white dwarf polarization at lick and keck observatories* (2025), arXiv:2504.12377 [hep-ph].
- [37] O. Ning and B. R. Safdi, *Phys. Rev. Lett.* **134**, 171003 (2025).
- [38] I. A. Sulai, S. Kalia, A. Arza, I. M. Bloch, E. C. Muñoz, C. Fabian, M. A. Fedderke, M. Forseth, B. Garthwaite, P. W. Graham, W. Griffith, E. Helgren, K. Hermanson, A. Interiano-Alvarado, B. Karki, *et al.*, *Phys. Rev. D* **108**, 096026 (2023).
- [39] A. Arza, M. A. Fedderke, P. W. Graham, D. F. Jackson Kimball, and S. Kalia, *Phys. Rev. D* **105**, 095007 (2022).
- [40] M. Friel, J. W. Gjerloev, S. Kalia, and A. Zamora, *Phys. Rev. D* **110**, 115036 (2024).
- [41] A. Nishizawa, A. Taruya, and Y. Himemoto, *Axion dark matter search from terrestrial magnetic fields at extremely low frequencies* (2025), arXiv:2504.07559 [hep-ph].
- [42] W. DeRocco and A. Hook, *Phys. Rev. D* **98**, 035021 (2018).
- [43] K. Nagano, T. Fujita, Y. Michimura, and I. Obata, *Phys. Rev. Lett.* **123**, 111301 (2019).
- [44] K. Nagano, H. Nakatsuka, S. Morisaki, T. Fujita, Y. Michimura, and I. Obata, *Phys. Rev. D* **104**, 062008 (2021).
- [45] J. Heinze, A. Gill, A. Dmitriev, J. c. v. Smetana, T. Yan, V. Boyer, D. Martynov, and M. Evans, *Phys. Rev. Lett.* **132**, 191002 (2024).
- [46] H. Liu, B. D. Elwood, M. Evans, and J. Thaler, *Phys. Rev. D* **100**, 023548 (2019).
- [47] S. Pandey, E. D. Hall, and M. Evans, *Phys. Rev. Lett.* **133**, 111003 (2024).
- [48] I. Obata, T. Fujita, and Y. Michimura, *Phys. Rev. Lett.* **121**, 161301 (2018).
- [49] Y. Oshima, H. Fujimoto, J. Kume, S. Morisaki, K. Nagano, T. Fujita, I. Obata, A. Nishizawa, Y. Michimura, and M. Ando, *Phys. Rev. D* **108**, 072005 (2023).
- [50] D. Martynov and H. Miao, *Phys. Rev. D* **101**, 095034 (2020).
- [51] H. Fujimoto, Y. Oshima, M. Ando, T. Fujita, Y. Michimura, K. Nagano, and I. Obata, *J. Phys. Conf. Ser.* **2156**, 012182 (2021).
- [52] G. Bertone, D. Hooper, and J. Silk, *Phys. Rep.* **405**, 279 (2005).
- [53] M. Weber and W. de Boer, *AA* **509**, A25 (2010).
- [54] R. Catena and P. Ullio, *J. Cosmol. Astropart. Phys.* **2010** (08), 004.
- [55] D. Budker, P. W. Graham, M. Ledbetter, S. Rajendran, and A. O. Sushkov, *Phys. Rev. X* **4**, 021030 (2014).
- [56] P. Zorabedian and W. R. Trutna, *Opt. Lett.* **13**, 826 (1988).

- [57] X. Baillard, A. Gauguier, S. Bize, P. Lemonde, P. Laurent, A. Clairon, and P. Rosenbusch, *Opt. Commun.* **266**, 609 (2006).
- [58] R. W. P. Drever, J. L. Hall, F. V. Kowalski, J. Hough, G. M. Ford, A. J. Munley, and H. Ward, *Appl. Phys. B* **31**, 97 (1983).